Check for updates

Molecular recognition of an acyl-peptide hormone and activation of ghrelin receptor

Yue Wang[1,2,7], Shimeng Guo[3,4,7], Youwen Zhuang[1,7], Ying Yun[2,4,7], Peiyu Xu [1,2,7], Xinheng He [1,2], Jia Guo[1,2], Wanchao Yin [1], H. Eric Xu [1,2,3,5✉], Xin Xie [2,3,4,5,6✉] & Yi Jiang [1,2✉]

Ghrelin, also called "the hunger hormone", is a gastric peptide hormone that regulates food intake, body weight, as well as taste sensation, reward, cognition, learning and memory. One unique feature of ghrelin is its acylation, primarily with an octanoic acid, which is essential for its binding and activation of the ghrelin receptor, a G protein-coupled receptor. The multi-faceted roles of ghrelin make ghrelin receptor a highly attractive drug target for growth retardation, obesity, and metabolic disorders. Here we present two cryo-electron microscopy structures of G_q-coupled ghrelin receptor bound to ghrelin and a synthetic agonist, GHRP-6. Analysis of these two structures reveals a unique binding pocket for the octanoyl group, which guides the correct positioning of the peptide to initiate the receptor activation. Together with mutational and functional data, our structures define the rules for recognition of the acylated peptide hormone and activation of ghrelin receptor, and provide structural templates to facilitate drug design targeting ghrelin receptor.

[1] CAS Key Laboratory of Receptor Research, Center for Structure and Function of Drug Targets, Shanghai Institute of Materia Medica, Chinese Academy of Sciences, Shanghai, China. [2] University of Chinese Academy of Sciences, Beijing, China. [3] School of Chinese Materia Medica, Nanjing University of Chinese Medicine, Nanjing, China. [4] CAS Key Laboratory of Receptor Research, National Center for Drug Screening, Shanghai Institute of Materia Medica, Chinese Academy of Sciences, Shanghai, China. [5] School of Life Science and Technology, ShanghaiTech University, Shanghai, China. [6] School of Pharmaceutical Science and Technology, Hangzhou Institute for Advanced Study, University of Chinese Academy of Sciences, Hangzhou, China. [7] These authors contributed equally: Yue Wang, Shimeng Guo, Youwen Zhuang, Ying Yun, Peiyu Xu. ✉email: eric.xu@simm.ac.cn; xxie@simm.ac.cn; yijiang@simm.ac.cn

Food intake is one of the most fundamental processes required for sustaining human life. It is primarily regulated by two endogenous hormones with opposite physiological functions: leptin, the energy surfeit hormone, and ghrelin, the hunger hormone, both of which are involved in controlling energy balance and obesity. Ghrelin is an orexigenic peptide hormone secreted from stomach in response to fasting situations and stimulates the ghrelin receptor in the brain to initiate appetite[1–4]. One unique feature of ghrelin is the fatty acid modification, with its third amino acid Ser[3] being modified with an octanoyl group[1], catalyzed by ghrelin O-acyltransferase (GOAT)[5,6]. Although less than 10% of ghrelin is acylated in the blood[7], this acyl-modification is essential for its activity. Both ghrelin and synthesized growth hormone secretagogues show potent growth hormone-releasing activity and serve as potential candidates for the treatment of growth hormone deficiency (GHD)[8]. The growth hormone-releasing activity also makes these hormones attractive performance-enhancing substances, whose usages are banned by the World Anti-Doping Agency in competitive sports[9].

The pleiotropic functions of ghrelin are mediated through the ghrelin receptor, also known as the growth hormone secretagogue receptor, which was first identified in the pituitary gland and the hypothalamus. As a G protein-coupled receptor (GPCR), the ghrelin receptor couples to G_q protein and modulates diverse physiological processes upon binding to ghrelin and other synthetic agonists[10]. LEAP2, an intestinally derived hormone, is identified as an endogenous antagonist of the ghrelin receptor, which fine-tunes ghrelin action via an endogenous counter-regulatory mechanism[11]. Ghrelin receptor is characterized by its high basal activity, with approximately 50% of its maximal capacity in the absence of a ligand[12,13]. This high level of basal activity may serve as a "signaling set point" to counterbalance the inhibitory input from leptin and insulin in appetite regulation[12]. Several naturally occurring mutations of *ghrelin receptor*, such as A204E and F279L, decrease the basal activity of the receptor and have been found to associate with obesity, diabetes, and short stature[14], which led to the idea of ghrelin receptor being an attractive therapeutic target for these diseases. However, there are only two orally active synthetic agonists, pralmorelin and macimorelin, been approved as diagnostic agents for GHD to date.

Extensive efforts have been devoted to examining the structural basis for the potential binding sites of ghrelin and synthetic agonists[13,15–19] and the basal activity of ghrelin receptor[20–22]. Nevertheless, compared to leptin and its receptor, which structures are known[23,24], much less are known about the structures of ghrelin and ghrelin-bound receptor. In this study, we reported two cryo-electron microscopy (cryo-EM) structures of the active ghrelin receptor–G_q complexes bound to ghrelin and GHRP-6, respectively.

Results

Structural determination. We fused thermostabilized BRIL at the N-terminus of the ghrelin receptor and applied the NanoBiT tethering strategy to improve complex stability and homogeneity (Supplementary Fig. 1a, b)[25]. These modifications have little effect on the pharmacological properties of the ghrelin receptor (Supplementary Fig. 2). An engineered $G\alpha_q$ was designed based on the mini-$G\alpha_s$ scaffold with its N-terminus replaced by corresponding sequences of $G\alpha_{i1}$ to facilitate the binding of scFv16 (Supplementary Fig. 1c), and such an analogous approach had been used to obtain structures of the G_q-bound 5-HT$_{2A}$ receptor[26] and G_{11}-bound M1 receptor[27]. Unless otherwise specified, G_q refers to the engineered G_q, which is used for further structure study. The ghrelin receptor was co-expressed with $G\alpha_q$ and $G\beta\gamma$, and

incubated with ghrelin in the presence of Nb35 to stabilize the receptor-G protein complex[28], allowing the efficient assembly of the ghrelin receptor–G_q complex. The scFv16 was additionally added to assemble the GHRP-6–ghrelin receptor–G_q–scFv16 complex (Supplementary Fig. 3).
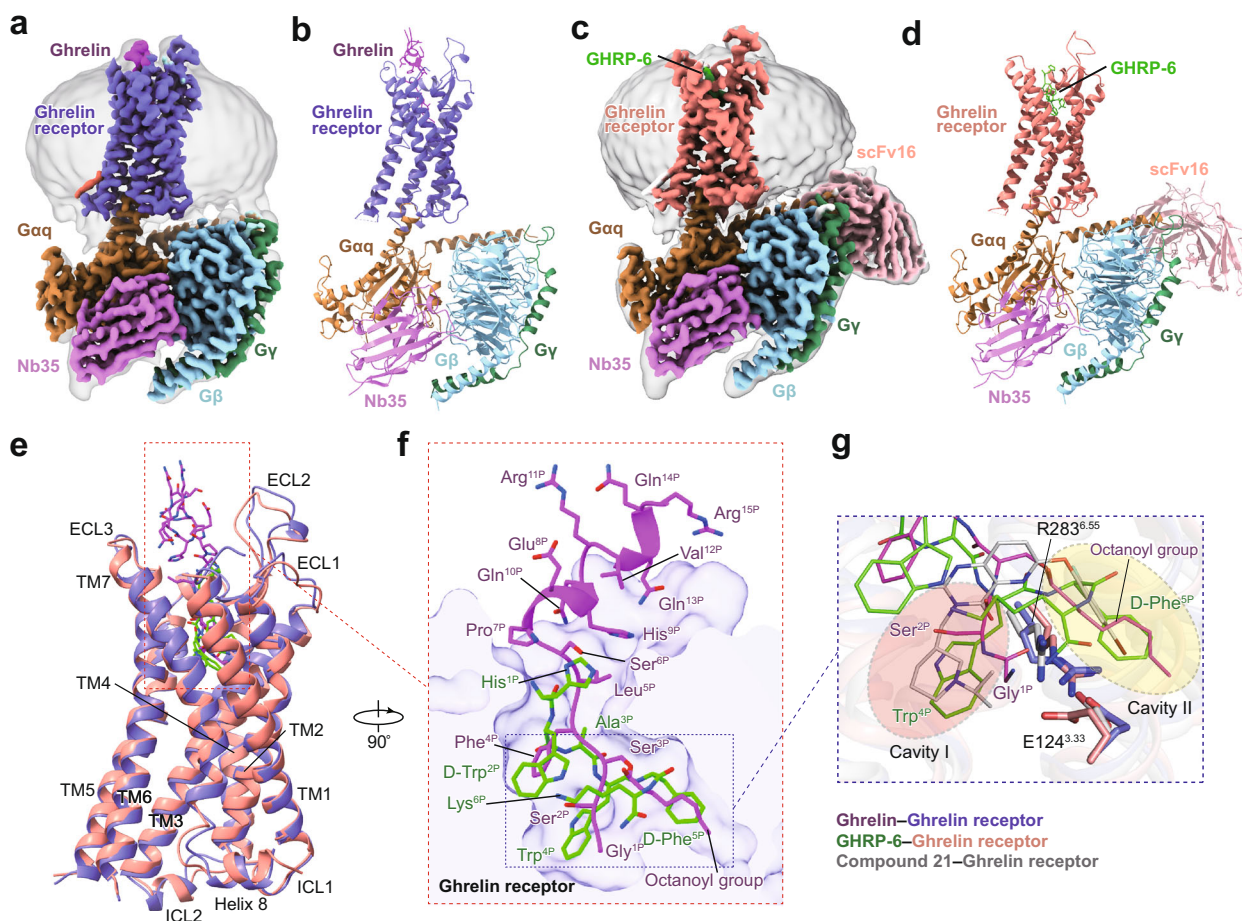
The complex structures of the G_q-coupled ghrelin receptor bound to ghrelin and GHRP-6 were determined by cryo-EM to the resolutions of 2.9 Å and 3.2 Å, respectively (Fig. 1a–d, Supplementary Fig. 3, Supplementary Table 1). For both ghrelin receptor–G_q complexes, the majority of the amino acid side chains of receptor and G_q protein were well-resolved in the final models, which are refined against the EM density map with excellent geometry. Both peptides, ghrelin (Gly^{1P}-Arg^{15P}) with octanoylated modification and GHRP-6, were clearly identified, thus providing reliable models for the mechanistic explanation of peptide recognition and activation of ghrelin receptor (Supplementary Fig. 4).

Overall structures of G_q-coupled ghrelin receptor bound to ghrelin and GHRP-6. Both ghrelin–ghrelin receptor–G_q and GHRP-6–ghrelin receptor–G_q complexes present canonical folds of seven transmembrane segments with the TMD of the receptors surrounded by an annular detergent micelle mimicking the natural phospholipid bilayer (Fig. 1a–d). Within the micelle, two cholesterols are clearly visible and hydrophobically bind around the helix bundles of both ghrelin receptor complexes. Both complexes display highly identical overall conformations with the root mean square deviation (RMSD) of 0.8 Å for entire complexes and 0.6 Å for ghrelin receptors (Fig. 1e). Ghrelin and GHRP-6 occupy the same orthosteric ligand-binding pocket of ghrelin receptor, comprising of all TM helices and extracellular loops (ECLs) except TM1 and ECL1 (Fig. 1e, Supplementary Fig. 5). The N-terminus of ghrelin inserts deep in the helix bundle. Conversely, GHRP-6 adopts an upside-down binding mode relative to ghrelin, with its C-terminus inserting into the helix bundle and its N-terminus facing the extracellular vestibule (Fig. 1f). Additionally, GHRP-6 is largely overlaid with the first six amino acids fragment of ghrelin (Fig. 1f). Recently, the structure of the ghrelin receptor bound to an antagonist compound 21 revealed a characteristic feature that the binding pocket is bifurcated into two cavities by a salt bridge between E124$^{3.33}$ and R283$^{6.55}$ [18]. Both ghrelin and GHRP-6 adopt similar binding modes and are buried in two identical cavities relative to compound 21, revealing a conserved binding pose for both peptidic agonists and antagonists (Fig. 1g).

Molecular basis for recognition of ghrelin by ghrelin receptor. The N-terminal amino acids from Gly^{1P} to Pro^{7P} of ghrelin occupied nearly the entire receptor TMD binding pocket (Fig. 2a). The peptide fragment from Glu^{8P} to Arg^{15P} is enriched with polar and charged amino acids and adopts an α-helical conformation, which sits above the orthosteric pocket and interacts with the solvent (Fig. 2a).

The clearly visible map allows us to locate Ser^{3P} and its octanoyl group accurately. A density connects the side-chain of Ser^{3P} and stretches horizontally toward the gap between TM4 and TM5, occupying cavity II of the binding pocket. Five carbons of the eight-carbon fatty acid modification can be placed in the density (Fig. 2b). F286$^{6.58}$ covers the side-chain of Ser^{3P}, while the fatty acid chain of ghrelin forms hydrophobic contacts with I178$^{4.60}$ and L181$^{4.63}$ (Figs. 2b, 3e). Most substitutions of I178$^{4.60}$, L181$^{4.63}$, and F286$^{6.58}$ with alanine or polar and charged amino acids (Ser, Asp, or Lys) display dramatically diminished receptor activation compared with wild-type (WT) ghrelin receptor (Fig. 2c, Supplementary Table 2). It is worth noting that

Fig. 1 Cryo-EM structures of the G$_q$-coupled ghrelin receptor bound to ghrelin and GHRP-6. a, **b** Orthogonal views of the density map (**a**) and model (**b**) for the ghrelin–ghrelin receptor–G$_q$–Nb35 complex. The density map is shown at 0.104 threshold. **c**, **d** Orthogonal views of the density map (**c**) and model (**d**) for the GHRP-6–ghrelin receptor–G$_q$–Nb35–scFv16 complex. The density map is shown at 0.1 threshold. **e** Structural superposition of ghrelin-bound and GHRP-6-bound ghrelin receptors. **f** Binding poses of ghrelin and GHRP-6. Two peptides occupy a similar orthosteric binding pocket with opposite orientation. **g** Binding pocket of ghrelin receptor is bifurcated into two cavities by a salt bridge between E124$^{3.33}$ and R283$^{6.55}$. Salmon oval, cavity I; yellow oval, cavity II. Ghrelin is shown in magenta, ghrelin-bound ghrelin receptor in slate blue. GHRP-6 is displayed in green, and GHRP-6 bound ghrelin receptor in salmon. Compound 21-bound ghrelin receptor (PDB: 6KO5) is colored gray. The G$_q$ heterotrimer is colored by subunits. Gα_q: peru, Gβ: light sky blue, Gγ: sea green, Nb35: orchid, scFv16: light pink.

F286$^{6.58}$ makes a greater contribution to ghrelin's activity. Mutating F286$^{6.58}$ to Asp produces an over 250-fold decreased activity of ghrelin (Fig. 2c), while mutating L178$^{4.60}$ or I181$^{4.63}$ to Asp diminishes the activities by only ~5-fold and 20-fold, respectively (Fig. 2c, Supplementary Table 2). These findings highlight the critical role of the potent receptor hydrophobic environment for binding of the octanoyl group. These results are consistent with the previous report that replacement of Ser^{3P} by a charged amino acid (Lys) or small hydrophobic residues (Val, Leu, or Ile) significantly decreased ghrelin's activity[29]. Conversely, replacing Ser^{3P} with aromatic amino acids, such as Trp or β-Nal (2-naphtylalanine), preserved ghrelin's activity[29].

Besides these hydrophobic residues surrounding the octanoyl group, other pocket residues also make substantial contributions to ghrelin binding and receptor activation. R283$^{6.55}$ forms a stabilizing salt bridge with E124$^{3.33}$ to lock TM3 and TM6 (Fig. 2b). Alanine mutations of E124$^{3.33}$ and R283$^{6.55}$ nearly abolished the binding of ghrelin-A2 and the ghrelin-induced receptor activity, indicating the critical role of the salt bridge in maintaining the integrity of the bifurcated binding pockets, and thus affecting ghrelin binding and receptor activation (Supplementary Figs. 6, 7b, Supplementary Table 2). Gly^{1P} and Ser^{2P} locate in cavity I of the ghrelin receptor binding pocket (Fig. 2d).

The main chain CO group of Ser^{2P} forms an H-bond with the side-chain of R102$^{2.63}$, which is critical for ghrelin binding (Fig. 2d, Supplementary Figs. 6, 7, Supplementary Table 2). Meanwhile, the N-terminal amino acid Gly^{1P} engages hydrophobic interactions with F279$^{6.51}$ and F312$^{7.42}$, which sit at the bottom of the binding pocket (Fig. 2d). It should be noted that alanine mutations of F279$^{6.51}$ and F312$^{7.42}$ partly maintain the binding of ghrelin but remarkably diminish its activity, indicating that these phenylalanines are mainly responsible for signal transmission (Fig. 2d, Supplementary Figs. 6, 7b, Supplementary Table 2). This finding suggests that the insertion of the octanoyl group into cavity II not only contributes to the binding of the ligand, but also helps to orient the N-terminus of ghrelin to cavity I, which is critical in receptor activation.

Additionally, Phe^{4P} is surrounded by hydrophobic residues, including L37$^{N\_Term}$, F38$^{N\_Term}$, L103$^{2.64}$, and F309$^{7.39}$, all contributing to ghrelin binding and its activity (Fig. 2e; Supplementary Figs. 6, 7b, Supplementary Table 2). Furthermore, Leu^{5P} forms an H-bond with Q302$^{7.32}$ via its main chain, while Ser^{6P} connects to ECL2 by forming an H-bond with E197^{ECL2}, both residues contribute to ghrelin binding (Figs. 2e, 3e, Supplementary Figs. 6, 7b, Supplementary Table 2). These detailed structural analyses provide insights to understand the
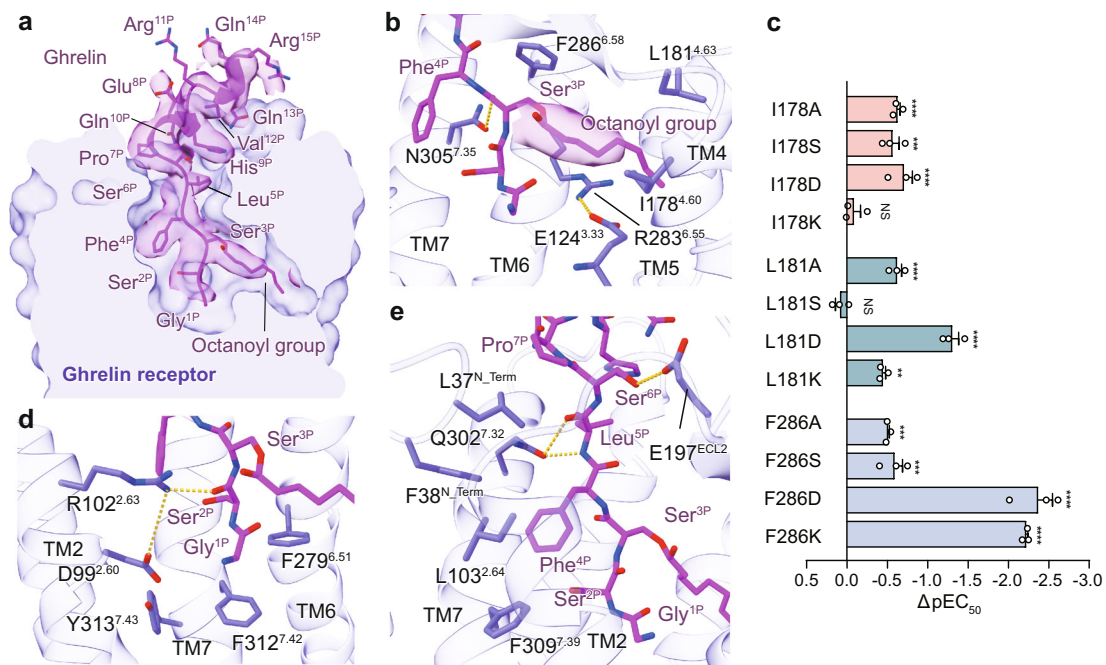
Fig. 2 The ghrelin-binding pocket of ghrelin receptor. a Cross-section of the ghrelin-binding pocket in ghrelin receptor. The cryo-EM density of ghrelin is highlighted. Ghrelin is shown in cartoon presentation. Side chains of the residues are displayed as sticks. **b** The binding pocket for octanoyl group. The cryo-EM density of the octanoyl group is shown. The hydrogen bonds are depicted as yellow dashed lines. **c** Effects of mutations of residues in the octanoyl group-binding pocket on calcium response. $\Delta pEC50$ represents the difference between pEC_{50} values of the mutant ghrelin receptor and the wild-type (WT) receptor. Data are presented as mean ± S.E.M. of three independent experiments performed in technical triplicate. ***$P < 0.001$, ****$P < 0.0001$ vs. WT receptor, NS, no significant difference. All data were analyzed by two-side, one-way ANOVA with Tukey's test ($P < 0.0001$, $P = 0.0002$, $P < 0.0001$, $P = 0.9871$, $P < 0.0001$, $P = 0.9888$, $P < 0.0001$, $P = 0.0028$, $P = 0.0006$, $P = 0.0001$, $P < 0.0001$, and $P < 0.0001$ from top to bottom). **d, e** Detailed interactions of ghrelin (Gly1P-Pro7P) with residues in ghrelin-binding pocket. Ghrelin is shown in magenta, and ghrelin receptor in slate blue.

recognition mechanism of the acyl-modified ghrelin by ghrelin receptor.

**Molecular basis for recognition of GHRP-6 by ghrelin receptor.** GHRP-6, a synthetic peptidic growth hormone secretagogue derived from met-enkephalin, shows no sequence homology with ghrelin[30]. It is buried in the same orthosteric site of the ghrelin receptor and displays comparable potency for receptor activation (Fig. 3a, Supplementary Fig. 7a). GHRP-6 adopts a similar binding pose with Gly1P-Ser6P of ghrelin (Fig. 1f). Cavity I accommodates Trp4P of GHRP-6 and offers a more extensive hydrophobic environment comprising F279[6.51], F309[7.39], F312[7.42], and Y313[7.43], of which F279[6.51] and Y313[7.43] are closely related to the activity of GHRP-6 (Figs. 1g, 3b, 3e, Supplementary Fig. 7c, Supplementary Table 2). D-Phe5P occupies cavity II and is highly overlaid with the entire octanoyl group of ghrelin (Figs. 1f, 3c). Besides its hydrophobic contacts with I178[4.60], L181[4.63], and F286[6.58], D-Phe5P forms an extra cation-π interaction with R283[6.55] relative to ghrelin (Fig. 3c). Although alanine substitutions of I178[4.60], L181[4.63], and F286[6.58] all significantly impair activities of ghrelin and GHRP-6, these residues make distinct extents of contributions. In contrast to ghrelin, replacement of I178[4.60] or L181[4.63] by alanine demonstrates a more remarkable decreased GHRP-6's activity than F286[6.58] (Fig. 3d, Supplementary Table 2).

In addition, D-Trp2P forms an edge-to-face packing with Trp4P and establishes a stabilizing intramolecular hydrophobic network with the side-chain of Lys6P (Fig. 3b). A previous study reported that growth hormone secretagogue metabolites without Lys6P abolished its ghrelin receptor binding capacity[8]. This finding is consistent with our observation that the side-chain of Lys6P points to TM2 and forms a stabilizing salt bridge with D99[2.60],

which is closely related to ghrelin receptor activation (Figs. 3b, e, Supplementary 7c, Supplementary Table 2). Our structural finding highlights the significance of Lys6P on GHRP-6's activity. Together, these results reveal the recognition mechanism of GHRP-6 and diversify the peptide-binding mode for ghrelin receptor.

Activation mechanism of ghrelin receptor. Structural comparison of two G_q-coupled ghrelin receptors with other $G_{q/11}$-coupled class A GPCRs reveals similar receptor conformations. TM6 and TM7 of ghrelin receptor adopt nearly identical conformations to G_q-coupled 5-HT$_{2A}$ receptor and G_{11}-coupled M1 receptor (Supplementary Fig. 8a, b). Unlike M1R, the cytoplasmic end of TM5 of the ghrelin receptor does not show an inward movement (Supplementary Fig. 8a). In addition, the Gα α5 helix displays slightly shifts and the distal end of Gα$_q$ α5 helix shows more notable shifts across these receptor complexes (Supplementary Fig. 8c). Furthermore, structural comparison of two G_q-coupled ghrelin receptors with the antagonist-bound ghrelin receptor (PDB: 6KO5)[18] supports the contention that these two complexes are indeed in the active state (Fig. 4a, b). These two ghrelin receptor complexes display pronounced outward displacements of TM6 cytoplasmic end (~8 Å, measured at Cα of H258[6.30]), the hallmark of GPCR activation, and ~3 Å inward shift of cytoplasmic end of TM7 (measured at Cα of Y323[7.53]) (Fig. 4a, b).

Although ghrelin and GHRP-6 differ in their chemical scaffolds, they induce the activation of ghrelin receptor through similar conformational changes in TM6 as well as TM7. Compared to the antagonist-bound receptor, the extracellular end of TM7 of these two active receptors laterally move ~5 Å towards TM6 (measured at Cα of Q302[7.32]), presenting a unique
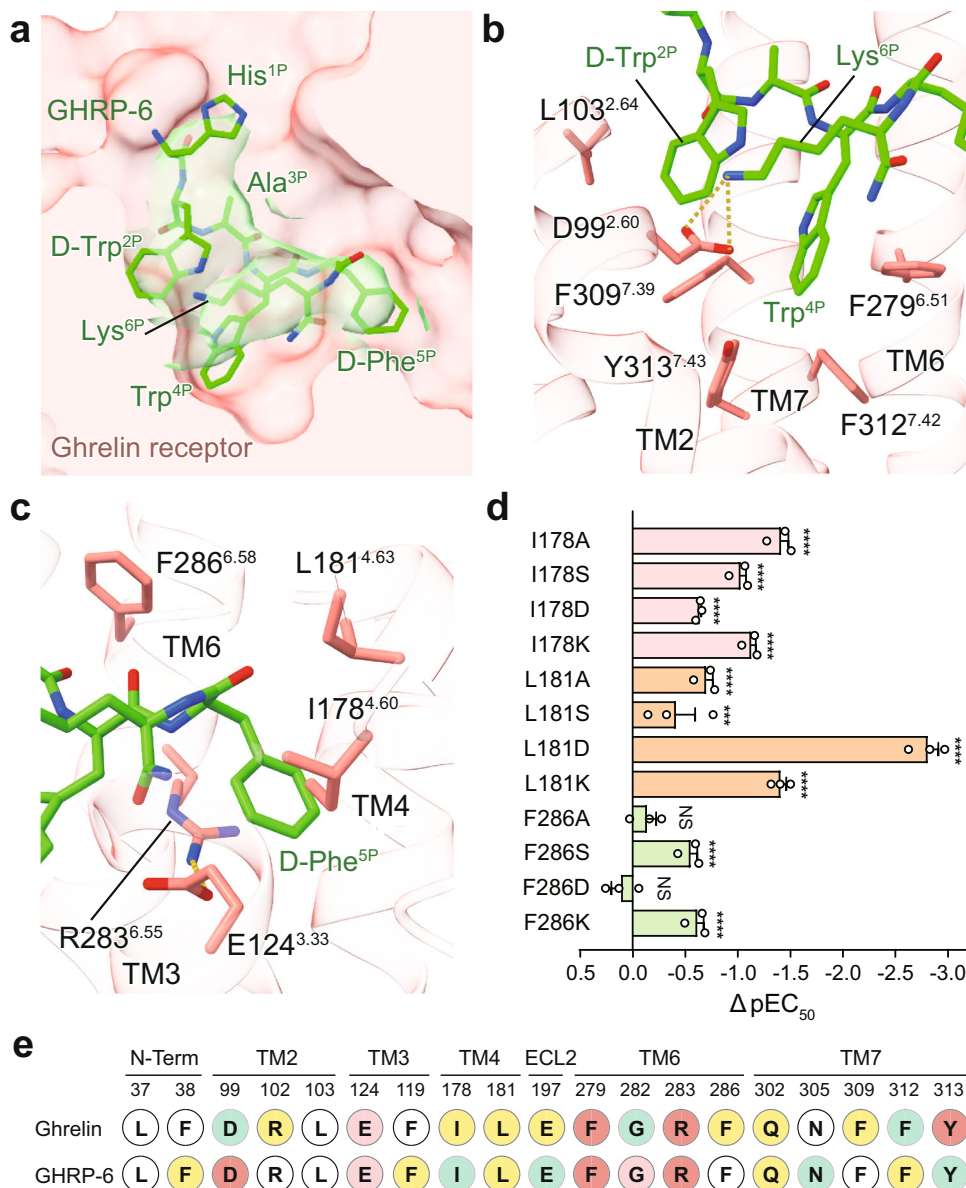
Fig. 3 The GHRP-6-binding pocket of ghrelin receptor. a Cross-section of the GHRP-6-binding pocket in ghrelin receptor. The cryo-EM density of GHRP-6 is highlighted. GHRP-6 is shown in a cartoon presentation. Side chains of the residues are displayed as sticks. **b**, **c** Detailed interactions of GHRP-6 with residues in GHRP-6 binding pocket. The binding site of D-Trp^{2P}, Trp^{4P}, Lys^{6P} (**b**) and D-Phe^{5P} (**c**) are shown. The hydrogen bond is depicted as a yellow dashed line. GHRP-6 is shown in green, and ghrelin receptor in salmon. **d** Effects of mutations of residues in D-Phe^{5P} binding pocket on calcium response. ΔpEC50 represents the difference between pEC$_{50}$ values of the mutant ghrelin receptor and the wild-type (WT) receptor. Data are presented as mean ± S.E.M. of three independent experiments performed in technical triplicate. $^{***}P < 0.001$, $^{****}P < 0.0001$ vs. WT receptor, NS, no significant difference. All data were analyzed by two-side, one-way ANOVA with Tukey's test ($P < 0.0001$, $P < 0.0001$, $P < 0.0001$, $P < 0.0001$, $P < 0.0001$, $P = 0.0009$, $P < 0.0001$, $P < 0.0001$, $P = 0.6335$, $P < 0.0001$, $P = 0.8310$, and $P < 0.0001$ from top to bottom). **e** Interaction residues in the ligand-binding pocket of the ghrelin–ghrelin receptor–G$_q$ and the GHRP-6–ghrelin receptor–G$_q$ complexes. Compared with WT receptor, the alanine replacement of residues showed comparable impacts on peptide's activity are indicated by white circles. The alanine mutation of residues showed 2-10-fold, 10-100-fold, 100-1000-fold, and over 1000-fold decreased peptide's activity are indicated by yellow, green, pink, and salmon circles, respectively.

TM7 conformational change across class A GPCRs solved to date (Fig. 4a, Supplementary Fig. 9). The notable movement of the extracellular end of TM7 may translate to the inward shift of its cytoplasmic end. Furthermore, structural comparison of both active and antagonist-bound receptors supports that R283$^{6.55}$ is the determinant for peptide-induced ghrelin receptor activation. The salt bridge between R283$^{6.55}$ and E124$^{3.33}$ exists in both antagonist-bound and active ghrelin receptor structure, however, in contrast to antagonist compound 21, ghrelin or GHRP-6 pushes the side-chain of R283$^{6.55}$ to swing away from the receptor

helical core, which induces rotation of TM6 that initiates the cascade of conformational changes in receptor activation (Fig. 4c, d). Concomitantly, the swing of R283$^{6.55}$ leads to the rotameric switches of F279$^{6.51}$ and W276$^{6.48}$, a residue in conserved "micro-switch". These conformational changes lead to the swing of F272$^{6.44}$ and the pronounced outward displacement of the cytoplasmic end of TM6 (Fig. 4e). The other conserved residues in "micro-switches" (ERY, PIF, and NPxxY) also undergo active-like conformational changes relative to the antagonist-bound receptor and transmit the peptidic agonism
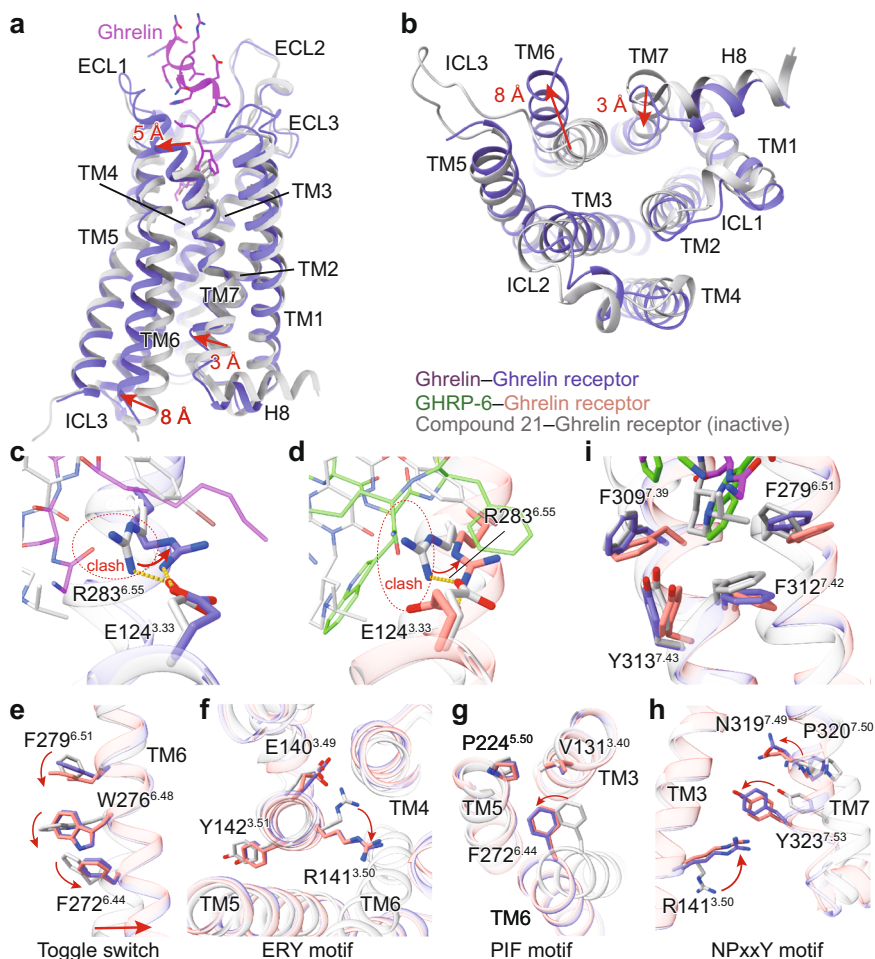
Fig. 4 Activation mechanism of ghrelin receptor. a, **b** Structural superposition of the active and antagonist-bound ghrelin receptor. (**a**) side view; (**b**) cytoplasmic view. **c**, **d** Conformational changes of the salt bridge comprising of E124$^{3.33}$ and R283$^{6.55}$ upon peptide activation. Ghrelin and GHRP-6 push the side-chain of R283$^{6.55}$ to swing away from the receptor helical core due to steric clash. The swing orientations of E124$^{3.33}$ and R283$^{6.55}$ were indicated by red arrows. The clashes were highlighted as red oval dashed lines. **e-h** Conformational changes of the conserved "micro-switches" upon receptor activation. (**e**) Toggle switch, (**f**) ERY motif, (**g**) PIF motif, (**h**) NPxxY motif. The outward displacement of TM6 of the active receptor is shown as a red arrow (**e**). The conformational changes of residue side chains are shown as red arrows upon receptor activation. **i** The hydrophobic cluster comprising F279$^{6.51}$, F309$^{7.39}$, F312$^{7.42}$, and Y313$^{7.43}$ stabilizes the inter-helical hydrophobic contacts between TM6 and TM7. Ghrelin is shown in magenta, ghrelin-bound ghrelin receptor in slate blue. GHRP-6 is displayed in green, and GHRP-6 bound ghrelin receptor in salmon. The compound 21-bound ghrelin receptor (PDB: 6KO5), is colored in gray.

signaling to the cytoplasmic end to facilitate receptor-G protein coupling. (Fig. 4f-h). Meanwhile, the conformational changes of F279$^{6.51}$ and W276$^{6.48}$ also cause rotameric switches of F312$^{7.42}$ and Y313$^{7.43}$ and the repacking of the inter-helical hydrophobic contacts between TM6 and TM7, which leads to the inward shift of the cytoplasmic end of TM7 (Fig. 4i).

Our structures also provide clues for understanding the mechanism of the basal activity of the ghrelin receptor. The hydrophobic residues F279$^{6.51}$, F312$^{7.42}$, and Y313$^{7.43}$ are closely packed and form a "hydrophobic lock" to packing TM6 and TM7 (Fig. 4i). As aforementioned, these hydrophobic residues primarily transmit peptide agonism signaling with limited impact on peptide binding. This finding raises a hypothesis that this hydrophobic lock may be responsible for the basal activity of the receptor. This hypothesis is further supported by our mutagenesis analysis that substituting F279$^{6.51}$ and F312$^{7.42}$ with alanine dramatically diminishes the basal activity of ghrelin receptor (Supplementary Fig. 10). It should be noted that alanine mutated Y313$^{7.43}$ reduced the surface expression of the receptor. However, when adjusting mutant expression to a comparable WT receptor

level, the basal activity displays a similarly significant decrease (Supplementary Fig. 10). Additionally, alanine mutations of E124$^{3.33}$ and R283$^{6.55}$ also lead to the significantly diminished basal activity of the ghrelin receptor, indicating a potential role of the salt bridge formed by these residues in modulating the receptor's basal activity (Supplementary Fig. 10). Together, the "hydrophobic lock" and the salt bridge may be involved in the regulation of the ghrelin receptor's basal activity.

Discussion

Collectively, this study reveals the structural basis for recognition of ghrelin and GHRP-6 by ghrelin receptor and identifies the binding site for the octanoyl group of ghrelin. According to our structure, the octanoyl group is located at cavity II but not cavity I, which is different from the previous modeling studies[17–19]. With mutagenesis studies, we propose an acyl-modification driven ghrelin-binding model, in which the binding of octanoyl group in cavity II orients the N-terminus of ghrelin to cavity I, and leads to the initiation of signal transduction. Structural

comparisons of G_q-coupled ghrelin receptor bound to ghrelin and GHRP-6 with the antagonist-bound receptor reveal a unique receptor activation mechanism. The binding of peptides causes steric hindrance to push the side-chain of R283[6.55] swinging away from the helix core and initiates the rotation of TM6. Altogether, these findings enhance our understanding of the molecular basis for acyl-ghrelin recognition and activation of the ghrelin receptor and provide a framework for the drug design targeting the ghrelin receptor.

Methods

Construct cloning. The full-length human ghrelin receptor (residues 1–366) was sub-cloned into pFastBac1 vector with an N-terminal haemagglutinin signal peptide (HA) and His×10 tag followed by BRIL epitope, as well as LgBiT at the C-terminus to facilitate the protein expression and stability. The ghrelin receptor sequence had no additional mutations or loop deletions. The $G\alpha_q$ was designed into a multifunctional chimera based on mini-$G\alpha_s$ skeleton with G_{i1} N-terminus for the binding of Nb35 and scFv16, respectively. $G\alpha_q$, rat Gβ1 with C-terminal HiBiT connected with a 15 residues linker, bovine Gγ2 and Ric8A were cloned into pFastBac1 vector, respectively. All constructs were prepared using homologous recombination (CloneExpress One Step Cloning Kit, Vazyme).

Protein expression. We used the Bac-to-Bac baculovirus system (Thermo Fisher) in *Spodoptera frugiperda* (sf9) cells for expression. Cell cultures were grown in ESF 921 serum-free medium (Expression Systems) to a density of $3–4 \times 10^6$ cells/ml. Ghrelin receptor, $G\alpha_q$, rat Gβ1, bovine Gγ2 and Ric8A were co-infected at the ratio of 1:1:1:1:1. After infected by 48 h, the cells were harvested by centrifugation at 2000 rpm (Thermo Fisher, H12000) for 20 min and kept frozen at −80 °C for further usage.

Complex purification. Cell pellets were thawed at R.T. and resuspended in 20 mM HEPES pH 7.5, 100 mM NaCl, 10 mM MgCl₂, 5 mM CaCl₂, 2 mM KCl, 0.1 mM TCEP, supplemented with Protease Inhibitor Cocktail (TargetMol, 1 mL/100 mL suspension). ScFv16 was applied to stabilize GHRP-6–ghrelin receptor–G_q complex, and Nb35 was used to improve the stability of both ghrelin receptor–G_q complexes. The monomeric scFv16 and Nb35 were prepared as previously reported[28,31]. Both ghrelin receptor–G_q complexes were formed on the membrane in the presence of 10 μM ligands (ghrelin or GHRP-6, synthesized by GenScript) and treated with apyrase (25 mU/ml, NEB), Nb35-His (15 μg/ml), or scFv16 followed by incubation for 1 h at R.T. The suspension was then solubilized by 0.5% (w/v) lauryl maltose neopentyl glycol (LMNG, Anatrace) with 0.1% (w/v) cholesteryl hemisuccinate TRIS salt (CHS, Anatrace) for 3 h. Insoluble material was removed by centrifugation at 65,000 g for 40 min and the solubilized complex was incubated overnight at 4 °C with pre-equilibrated Nickel resin (Ni Smart Beads 6FF, SMART Lifesciences) containing 10 mM imidazole. The resin was washed with 15 column volumes of Wash Buffer 1 containing 20 mM HEPES pH 7.5, 100 mM NaCl, 2 mM MgCl₂, 15 mM imidazole, 0.1% LMNG, 0.02% CHS, 10 μM ligands (ghrelin or GHRP-6) and 15 column volumes of Wash Buffer 2 containing 20 mM HEPES, pH 7.5, 100 mM NaCl, 2 mM MgCl₂, 25 mM imidazole, 0.01% LMNG, 0.005% GDN (Anatrace), 0.003% CHS, 10 μM ligands (ghrelin or GHRP-6). The complex was then eluted with 5 column volumes of Elution Buffer containing 20 mM HEPES, pH 7.5, 100 mM NaCl, 250 mM imidazole, 2 mM MgCl₂, 0.01% LMNG, 0.005% GDN, 0.003% CHS and 10 μM ligands (ghrelin or GHRP-6). The complex was concentrated to 0.5 ml using Ultra Centrifugal Filter (Thermo-Fisher MWCO, 100 kDa) and subjected to size-exclusion chromatography on a Superdex 200 Increase 10/300 column (GE Healthcare) that was pre-equilibrated with 20 mM HEPES pH 7.5, 100 mM NaCl, 2 mM MgCl₂, 5 μM ligands, 0.00075% (w/v) LMNG, 000025% glyco-diosgenin (GDN, Anatrace) and 0.00015% (w/v) CHS to separate complex from contaminants. Eluted fractions that consisted of receptor and G protein complex were pooled and concentrated to approximately 10 mg/ml for electron microscopy experiments.

Cryo-EM grid preparation and data collection. For the cryo-EM grids preparation, 3 μl of purified ghrelin-bound complex at 13 mg/ml and GHRP-6-bound ghrelin receptor complex at 8 mg/ml were applied individually onto a glow-discharged holey carbon grid (Quantifoil, Au300 R1.2/1.3) in a Vitrobot chamber (FEI Vitrobot Mark IV). Cryo-EM imaging was performed on a Titan Krios at 300 kV accelerating voltage in the Center of Cryo-Electron Microscopy Research Center, Shanghai Institute of Materia Medica, Chinese Academy of Sciences (Shanghai, China). Micrographs were recorded using a Gatan K3 Summit direct electron detector in counting mode with a nominal magnification of ×81,000, which corresponds to a pixel size of 1.045 Å. Movies were obtained using serialEM at a dose rate of about 26.7 electrons per A² per second with a defocus ranging from −0.5 to −3.0 μm. The total exposure time was 3 s and intermediate frames were recorded in 0.083 s intervals, resulting in an accumulated dose of 80 electrons per A² and a total of 36 frames per micrograph. A total of 5673 and 3362 movies

were collected for the ghrelin-bound and GHRP-6-bound ghrelin receptor complex, respectively.

Cryo-EM data processing. Dose-fractionated image stacks for the ghrelin-bound ghrelin receptor–$G\alpha_q$ complex were subjected to beam-induced motion correction using MotionCor2.1[32]. Contrast transfer function (CTF) parameters for each micrograph were determined by Ctffind4[33]. Particle selection, 2D and 3D classifications of the ghrelin-bound ghrelin receptor–G_q complex were performed on a binned data set with a pixel size of 2.09 Å using RELION-3.0-beta2[34].

For the ghrelin-bound ghrelin receptor–$G\alpha_q$ complex, semi-automated particle selection yielded 4,598,528 particle projections. The projections were subjected to 2D classification to discard particles in poorly defined classes, producing 1,842,606 particle projections for further processing. The map of the D1R–G_s complex low-pass filtered to 40 Å was used as a reference model for four rounds of maximum-likelihood-based 3D classifications, resulting in one well-defined subset with 912,636 projections. A map generated by 3D refinement was subsequently post-processed in DeepEMhancer[35]. The final refinement generated a map with an indicated global resolution of 2.9 Å at a Fourier shell correlation of 0.143.

For the GHRP-6-bound ghrelin receptor–$G\alpha_q$ complex, semi-automated particle selection yielded 2,728,266 particle projections. The projections were subjected to 2D classification, producing 1,523,752 particle projections for further processing. The map of the D1R–G_s complex low-pass filtered to 40 Å was used as a reference model for three rounds of maximum-likelihood-based 3D classifications, resulting in two well-defined subsets with 262,892 projections. A map generated by 3D refinement was subsequently post-processed in DeepEMhancer[35]. The final refinement generated a map with an indicated global resolution of 3.2 Å at a Fourier shell correlation of 0.143. Local resolution for both density maps was determined using the Bsoft package with half maps as input maps[36].

Model building and refinement. The crystal structure of the ghrelin receptor (PDB: 6KO5) was used as an initial model for model rebuilding and refinement against the electron microscopy maps of ghrelin receptor–$G\alpha_q$ complexes. The structure of the G_q part of the 5-HT$_{2A}$ complex (PDB: 6WHA) was used as initial models for model building of the ghrelin/GHRP-6 bound ghrelin receptor–$G\alpha_q$–Nb35–(scFv16) complex. The initial models were docked into the electron microscopy density maps using Chimera[37] followed by iterative manual adjustment and rebuilding in COOT[38]. Real-space refinement and reciprocal space refinement were performed using Phenix programs[39]. The model statistics were validated using MolProbity[40]. Structure figures were prepared in Chimera and PyMOL (https://pymol.org/2/). The final refinement statistics are provided in Extended Data Table 1. The extent of any model overfitting during refinement was measured by refining the final model against one of the half-maps and by comparing the resulting map versus model FSC curves with the two half-maps and the full model.

Ligand-binding assays. Ligand binding was performed with a homogeneous time-resolved fluorescence-based assay. N-terminal-SNAP-tagged ghrelin receptor (WT or with various mutations) and full-length ghrelin labeled with the dye A2 on an additional cysteine at the C-terminal end of the peptide (ghrelin-A2, synthesized by Vazyme, China) were used as previously described[41].

HEK293 cells transfected with SNAP-ghrelin receptor (WT or mutants) were seeded at a density of 1×10^6 cells into 3 cm dish and incubated for 24 h at 37 °C in 5% CO₂. Cell culture medium was removed and Tag-lite labeling medium with 100 nM of SNAP-Lumi4-Tb (Cisbio, SSNPTBC) was added, and the cells were further incubated for 1 h at 37 °C in 5% CO₂. The excess of SNAP-Lumi4-Tb was then removed by washing 4 times with 1 ml of Tag-lite labeling medium.

For saturation binding experiments, we incubated cells with increasing concentrations of ghrelin-A2 in the presence or absence of 10 μM unlabeled ghrelin for 1 h at R.T. Signal was detected using the Multimode Plate Reader (PerkinElmer EnVision) equipped with an HTRF optic module allowing a donor excitation at 340 nm and a signal collection both at 665 nm and at 620 nm. HTRF ratios were obtained by dividing the acceptor signal (665 nm) by the donor signal (620 nm). Kd values were obtained from binding curves using Prism 8.0 software (GraphPad Software).

Calcium assay. The wild-type ghrelin receptor gene was sub-cloned in the pcDNA3.0 vector with an N-terminal HA signal peptide. Mutations were introduced by QuickChange PCR. All of the constructs were verified by DNA sequencing. HEK293 cells transfected with HA-tagged WT ghrelin receptor or mutants were seeded at a density of 4×10^4 cells per well into 96-well culture plates and incubated for 24 h at 37 °C in 5% CO₂. The cells were then incubated with 2 μmol/L Fluo-4 AM in HBSS (5.4 mmol/L KCl, 0.3 mmol/L Na₂HPO₄, 0.4 mmol/L KH₂PO₄, 4.2 mmol/L NaHCO₃, 1.3 mmol/L CaCl₂, 0.5 mmol/L MgCl₂, 0.6 mmol/L MgSO₄, 137 mmol/L NaCl, 5.6 mmol/L D-glucose and 250 μmol/L sulfinpyrazone, pH 7.4) at 37 °C for 40 min. After thorough washing, 50 μL of HBSS was added. After incubation at R.T. for 10 min, 25 μL of agonist was dispensed into the well using a FlexStation III microplate reader (Molecular Devices), and the intracellular

calcium change was recorded at an excitation wavelength of 485 nm and an emission wavelength of 525 nm. EC_{50} and E_{max} values for each curve were calculated by Prism 8.0 software.

Cell-surface expression assay. Cell-surface expression for each mutant was monitored by a fluorescence-activated cell sorting (FACS) assay. In brief, the expressed cells were incubated with mouse anti-HA-FITC antibody (Sigma) at a dilution of 1:200 for 20 min at 4 °C, and then a 9-fold excess of PBS was added to cells. Finally, the surface expression of the ghrelin receptor was monitored by detecting the fluorescent intensity of FITC using a BD ACCURI C6. The FACS data were analyzed by BD Accuri C6 software 1.0.264.21. The gating strategy and calculation method of expression are shown in Supplementary Fig. 11.

Inositol phosphate accumulation assay. IP1 production was measured using the IP-One HTRF kit (Cisbio, 621PAPEJ)[41]. Briefly, 24 h after transfection, cells were harvested and resuspended in PBS at a density of 4×10^6 cells/ml. Cells were then plated onto 384-well assay plates at 20,000 cells/5 μl/well. Another 5 μl IP1 stimulation buffer containing ligand was added to the cells, and the incubation lasted for 30 min at R.T. As a negative control, cells transfected with pcDNA3.0 empty vector were also tested. Intracellular IP1 measurement was carried with the IP-One HTRF kit and EnVision multiplate reader according to the manufacturer's instructions. The HTRF ratio was converted to a response (%) using the following formula: response (%) = (ratio of sample−ratio of the negative control)/(ratio of WT−ratio of the negative control) ×100.

Statistical analysis. All functional study data were analyzed using Prism 8 (GraphPad) and presented as means ± S.E.M. from at least three independent experiments. Concentration-response curves were evaluated with a three-parameter logistic equation. EC_{50} is calculated with the Sigmoid three-parameter equation. The significance was determined with two-side, one-way ANOVA with Tukey's test, and $P < 0.05$ vs. wild type (WT) was considered statistically significant.

Reporting summary. Further information on research design is available in the Nature Research Reporting Summary linked to this article.

Data availability
The atomic coordinates and the electron microscopy maps have been deposited in the Protein Data Bank (PDB) under accession number 7F9Y and 7F9Z and Electron Microscopy Data Bank (EMDB) accession number EMD-31500 and EMD-31501 for the ghrelin–ghrelin receptor–G_q–Nb35 and the GHRP-6–ghrelin receptor–G_q–scFv16–Nb35 complex, respectively. Source data are provided with this paper.

References
1. Kojima, M., Hosoda, H., Matsuo, H. & Kangawa, K. Ghrelin: discovery of the natural endogenous ligand for the growth hormone secretagogue receptor. *Trends Endocrinol. Metab.* **12**, 118–122 (2001).
2. Kojima, M. et al. Ghrelin is a growth-hormone-releasing acylated peptide from stomach. *Nature* **402**, 656–660 (1999).
3. Yanagi, S., Sato, T., Kangawa, K. & Nakazato, M. The homeostatic force of ghrelin. *Cell Metab.* **27**, 786–804 (2018).
4. Klok, M. D., Jakobsdottir, S. & Drent, M. L. The role of leptin and ghrelin in the regulation of food intake and body weight in humans: a review. *Obes. Rev.* **8**, 21–34 (2007).
5. Yang, J., Brown, M. S., Liang, G., Grishin, N. V. & Goldstein, J. L. Identification of the acyltransferase that octanoylates ghrelin, an appetite-stimulating peptide hormone. *Cell* **132**, 387–396 (2008).
6. Gutierrez, J. A. et al. Ghrelin octanoylation mediated by an orphan lipid transferase. *Proc. Natl Acad. Sci. USA* **105**, 6320–6325 (2008).
7. Patterson, M., Murphy, K. G., le Roux, C. W., Ghatei, M. A. & Bloom, S. R. Characterization of ghrelin-like immunoreactivity in human plasma. *J. Clin. Endocrinol. Metab.* **90**, 2205–2211 (2005).
8. Ferro, P., Krotov, G., Zvereva, I., Rodchenkov, G. & Segura, J. Structure-activity relationship for peptidic growth hormone secretagogues. *Drug Test. Anal.* **9**, 87–95 (2017).
9. Semenistaya, E. et al. Determination of growth hormone releasing peptides metabolites in human urine after nasal administration of GHRP-1, GHRP-2, GHRP-6, Hexarelin, and Ipamorelin. *Drug Test. Anal.* **7**, 919–925 (2015).
10. Howard, A. D. et al. A receptor in pituitary and hypothalamus that functions in growth hormone release. *Science* **273**, 974–977 (1996).
11. Ge, X. et al. LEAP2 Is an endogenous antagonist of the ghrelin receptor. *Cell Metab.* **27**, 461–469 e466 (2018).
12. Holst, B. & Schwartz, T. W. Constitutive ghrelin receptor activity as a signaling set-point in appetite regulation. *Trends Pharm. Sci.* **25**, 113–117 (2004).
13. Feighner, S. D. et al. Structural requirements for the activation of the human growth hormone secretagogue receptor by peptide and nonpeptide secretagogues. *Mol. Endocrinol.* **12**, 137–145 (1998).
14. Wang, W. & Tao, Y. X. Ghrelin receptor mutations and human obesity. *Prog. Mol. Biol. Transl. Sci.* **140**, 131–150 (2016).
15. Holst, B. et al. Overlapping binding site for the endogenous agonist, small-molecule agonists, and ago-allosteric modulators on the ghrelin receptor. *Mol. Pharm.* **75**, 44–59 (2009).
16. Holst, B. et al. Identification of an efficacy switch region in the ghrelin receptor responsible for interchange between agonism and inverse agonism. *J. Biol. Chem.* **282**, 15799–15811 (2007).
17. Bender, B. J. et al. Structural model of ghrelin bound to its G protein-coupled receptor. *Structure* **27**, 537–544 e534 (2019).
18. Shiimura, Y. et al. Structure of an antagonist-bound ghrelin receptor reveals possible ghrelin recognition mode. *Nat. Commun.* **11**, 4160 (2020).
19. Ferre, G. et al. Structure and dynamics of G protein-coupled receptor-bound ghrelin reveal the critical role of the octanoyl chain. *Proc. Natl Acad. Sci. USA* **116**, 17525–17530 (2019).
20. Holst, B. et al. Common structural basis for constitutive activity of the ghrelin receptor family. *J. Biol. Chem.* **279**, 53806–53817 (2004).
21. Mokrosinski, J., Frimurer, T. M., Sivertsen, B., Schwartz, T. W. & Holst, B. Modulation of constitutive activity and signaling bias of the ghrelin receptor by conformational constraint in the second extracellular loop. *J. Biol. Chem.* **287**, 33488–33502 (2012).
22. Goze, C. et al. Involvement of tryptophan W276 and of two surrounding amino acid residues in the high constitutive activity of the ghrelin receptor GHS-R1a. *Eur. J. Pharm.* **643**, 153–161 (2010).
23. Zhang, F. et al. Crystal structure of the obese protein leptin-E100. *Nature* **387**, 206–209 (1997).
24. Carpenter, B. et al. Structure of the human obesity receptor leptin-binding domain reveals the mechanism of leptin antagonism by a monoclonal antibody. *Structure* **20**, 487–497 (2012).
25. Duan, J. et al. Cryo-EM structure of an activated VIP1 receptor-G protein complex revealed by a NanoBiT tethering strategy. *Nat. Commun.* **11**, 4121 (2020).
26. Kim, K. et al. Structure of a hallucinogen-activated Gq-coupled 5-HT2A serotonin receptor. *Cell* **182**, 1574–1588 e1519 (2020).
27. Maeda, S., Qu, Q., Robertson, M. J., Skiniotis, G. & Kobilka, B. K. Structures of the M1 and M2 muscarinic acetylcholine receptor/G-protein complexes. *Science* **364**, 552–557 (2019).
28. Rasmussen, S. G. et al. Crystal structure of the beta2 adrenergic receptor-Gs protein complex. *Nature* **477**, 549–555 (2011).
29. Matsumoto, M. et al. Structure-activity relationship of ghrelin: pharmacological study of ghrelin peptides. *Biochem. Biophys. Res. Commun.* **287**, 142–146 (2001).
30. DeVita, R. J. Small molecule mimetics of GHRP-6. *Expert Opin. Investig. Drugs* **6**, 1839–1843 (1997).
31. Koehl, A. et al. Structure of the micro-opioid receptor-Gi protein complex. *Nature* **558**, 547–552 (2018).
32. Zheng, S. Q. et al. MotionCor2: anisotropic correction of beam-induced motion for improved cryo-electron microscopy. *Nat. Methods* **14**, 331–332 (2017).
33. Rohou, A. & Grigorieff, N. CTFFIND4: Fast and accurate defocus estimation from electron micrographs. *J. Struct. Biol.* **192**, 216–221 (2015).
34. Zivanov, J. et al. New tools for automated high-resolution cryo-EM structure determination in RELION-3. *Elife* 7, https://doi.org/10.7554/eLife.42166 (2018).
35. Sánchez-García, R. et al. DeepEMhacer: a deep learning solution for cryo-EM volume post-processing. *Commun. Biol.* **4**, 874 (2021).
36. Heymann, J. B. Guidelines for using Bsoft for high resolution reconstruction and validation of biomolecular structures from electron micrographs. *Protein Sci.* **27**, 159–171 (2018).
37. Pettersen, E. F. et al. UCSF Chimera—a visualization system for exploratory research and analysis. *J. Comput. Chem.* **25**, 1605–1612 (2004).
38. Emsley, P. & Cowtan, K. Coot: model-building tools for molecular graphics. *Acta Crystallogr. D: Biol. Crystallogr.* **60**, 2126–2132 (2004).
39. Adams, P. D. et al. PHENIX: a comprehensive Python-based system for macromolecular structure solution. *Acta Crystallogr. D: Biol. Crystallogr.* **66**, 213–221 (2010).
40. Chen, V. B. et al. MolProbity: all-atom structure validation for macromolecular crystallography. *Acta Crystallogr. D: Biol. Crystallogr.* 66, 12–21 (2010).
41. Leyris, J. P. et al. Homogeneous time-resolved fluorescence-based assay to screen for ligands targeting the growth hormone secretagogue receptor type 1a. *Anal. Biochem* **408**, 253–262 (2011).

Author contributions

Y.J., H.E.X., and X.X conceived, designed, and supervised the overall project. Y.J., H.E.X., X.X., Y.W., S.-M.G. Y.-W.Z., and P.-Y.X. participated in data analysis and interpretation; Y.W. generated the ghrelin receptor insect cell expression constructs, established the ghrelin–ghrelin receptor–G_q –Nb35 and GHRP-6–ghrelin receptor–G_q–Nb35 –scFv16 complex purification protocol and prepared samples for the cryo-EM as well as data collection; S.-M.G. and Y.Y. designed all of the mutants for the ligand-binding pockets and executed all the cellular experiments including the ligand-binding assay, Calcium assay and IP1 assay supervised by X.X.; Y.-W.Z. performed cryo-EM data processing and P.-Y.X. performed model building and refinement; X.-H.H. modeled disease-related mutants; J.G. assisted Y.W. with protein complex purification and sample preparation for cryo-EM; W.C.Y. designed G_q protein constructs; Y.J., Y.W., S.-M.G. prepared the figures; Y.J., H.E.X., X.X., Y.W., S.-M.G. wrote the manuscript with input from all authors.

Competing interests

The authors declare no competing interests.

Additional information

Supplementary information The online version contains supplementary material available at https://doi.org/10.1038/s41467-021-25364-2.

Correspondence and requests for materials should be addressed to H.E.X., X.X. or Y.J.

Peer review information *Nature Communications* thanks Birgitte Holst, Mohammed Hossain and the other, anonymous, reviewer(s) for their contribution to the peer review of this work.

Reprints and permission information is available at http://www.nature.com/reprints

Publisher's note Springer Nature remains neutral with regard to jurisdictional claims in published maps and institutional affiliations.